Eur. Phys. J. A **21**, 487–500 (2004)
DOI 10.1140/epja/i2004-10007-y

THE EUROPEAN PHYSICAL JOURNAL A

Nucleon-pole contributions in the $J/\psi \to N\bar{N}\pi$, $p\bar{p}\eta$, $p\bar{p}\eta'$ and $p\bar{p}\omega$ decays

W.-H. Liang[1,3], P.-N. Shen[2,1,4,a], B.-S. Zou[4,1,2], and A. Faessler[5]

[1] Institute of High Energy Physics, Chinese Academy of Sciences, P.O. Box 918(4), Beijing 100039, PRC
[2] China Center of Advanced Science and Technology (World Laboratory), P.O. Box 8730, Beijing 100080, PRC
[3] Department of Physics, Guangxi Normal University, Guilin 541004, PRC
[4] Center of Theoretical Nuclear Physics, National Laboratory of Heavy Ion Accelerator, Lanzhou 730000, PRC
[5] Institut für Theoretische Physik, Universität Tübingen, Auf der Morgenstelle 14, D-72076 Tübingen, Germany

Received: 2 March 2004 /
Published online: 27 September 2004 –
Communicated by V.V. Anisovich

Abstract. Nucleon-pole contributions in the $J/\psi \to N\bar{N}\pi$, $p\bar{p}\eta$, $p\bar{p}\eta'$ and $p\bar{p}\omega$ decays are re-studied. Different contributions due to PS-PS and PS-PV couplings in the π-N interaction and the effects of $NN\pi$ form factors are investigated in the $J/\psi \to N\bar{N}\pi$ decay channel. It is found that when the ratio of $|F_0|/|F_M|$ takes a small value, without considering the $NN\pi$ form factor, the difference between PS-PS and PS-PV couplings is negligible. However, when the $NN\pi$ form factor is included, this difference is greatly enlarged. The resultant decay widths are sensitive to the form factors. As a conclusion, the nucleon-pole contribution as a background to the decay width is important in the $J/\psi \to N\bar{N}\pi$ decay and must be considered. In the $J/\psi \to N\bar{N}\eta$ and $N\bar{N}\eta'$ decays, its contribution is smaller by 0.1% with respect to the data. In the $J/\psi \to N\bar{N}\omega$ decay, it provides a rather important contribution without considering form factors. But the contribution is suppressed greatly when adding the off-shell form factors. Comparing these results with data will help us to select a proper form factor for such kind of decay.

PACS. 14.20.Gk Baryon resonances with $S = 0$ – 13.25.Gv Decays of J/ψ, Υ, and other quarkonia – 13.66.Bc Hadron production in e^-e^+ interactions

1 Introduction

Nucleons, as essential building blocks of the real world, have been studied for decades. The members of the nucleon family include those which are in different excitation modes and even with gluon contents. The nucleon spectrum investigation will provide us necessary information for revealing the structure of the nucleon [1]. So far, in terms of a variety of sources, mostly from the πN elastic- and inelastic-scattering data, more and more information on nucleon and its excited states have been accumulated. However, our knowledge on the nucleon family is still far from complete.

The development of Quantum Chromodynamics (QCD) provides an underlying theory for the studies of hadrons and their properties. Even so, the nucleon and its family members still cannot strictly be derived from QCD. The difficulty comes from two sides: the interaction among quarks and the intrinsic structures of the nucleon and its family members. To solve this problem in a more efficient way, various QCD-inspired models have been proposed. As a result, many nucleon resonances (N^*) have been predicted.

On the experimental side, searching N^*'s has been a very important project in the past years. The results were mainly extracted from the πN scattering data. Up to now, many nucleon resonances have been found. Yet, still some N^* states which were predicted by widely accepted nucleon models, such as quark models [2], have not been seen in the πN channel. Do these so-called "missing resonances" couple weakly to the πN channel [3,4], so that we should propose other means to search them? Or, does the quark model predict too many resonances so that the model itself should further be modified? Or, may there exist the hybrid structure or the di-quark structure? All these puzzles motivate intensive investigations on both the experimental and the theoretical side.

In recent years, a large number of experiments on N^* physics have been carried out at new facilities such as CEBAF at JLab, ELSA at Bonn, GRAAL at Grenoble and

[a] e-mail: shenpn@mail.ihep.ac.cn

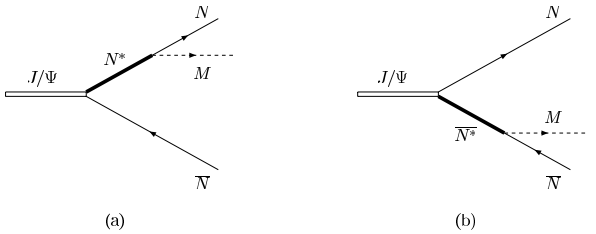

Fig. 1. N^*-pole diagrams for the $J/\psi \to MN\bar{N}$ decay.

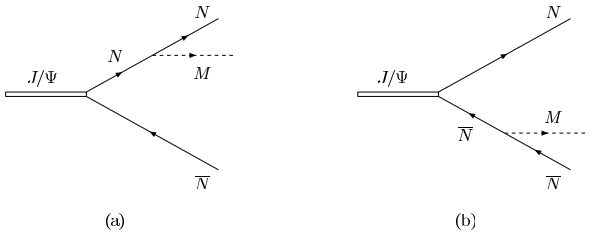

Fig. 2. Nucleon-pole diagrams for the $J/\psi \to MN\bar{N}$ decay.

SPring-8 at JASRI. Now, 58 million J/ψ events have been collected at Beijing Electron-Positron Collider (BEPC). The two-step decay process $J/\psi \to N^*\bar{N} \to MN\bar{N}$, where M stands for meson, can be another excellent source for studying light-baryon resonances with many advantages [5,6]. The corresponding Feynman diagrams are shown in fig. 1. It should be mentioned that the nucleon-pole diagrams (shown in fig. 2) could also contribute as a background component in the N^* study via $J/\psi \to MN\bar{N}$ decays. For light mesons, especially for pions, nucleon-pole contributions might be sizable and should not be ignored.

In order to extract a more accurate and reliable conclusion from the J/ψ hadronic-decay data, it is necessary to study the nucleon-pole contributions in those decay channels. By analyzing $J/\psi \to p\bar{p}\pi^0$ data, R. Sinha and S. Okubo [7] pointed out that in the $J/\psi \to p\bar{p}\pi^0$ decay, the p-pole contribution dominates in the soft-pion limit, and the N^*-pole contribution becomes important in the large pion energy region. In the $J/\psi \to p\bar{p}\eta$ and $p\bar{p}\eta'$ decays, if one considered the p-pole contribution only, the extracted $g_{\eta N\bar{N}}/g_{\pi N\bar{N}}$ value would be much smaller than that from the experimental decay widths of the $J/\psi \to p\bar{p}\pi^0$, $p\bar{p}\eta$ and $p\bar{p}\eta'$ processes. Due to the fact that the decay rates $\Gamma(N^* \to \eta N)$ are rather large for both $N^*(1440)$ and $N^*(1535)$, the N^*-pole contribution must govern $J/\psi \to p\bar{p}\eta$ and $p\bar{p}\eta'$ decays. In the $J/\psi \to p\bar{p}\omega$ decay, the p-pole contribution only gives 1/10 of the experimental decay rate. Therefore, in order to obtain a reliable information about N^* via $J/\psi \to p\bar{p}M$ decays, one should carefully consider the p-pole contribution as a part of the background component. In this work, we calculate the nucleon-pole contributions in the $J/\psi \to N\bar{N}\pi$, $p\bar{p}\eta$, $p\bar{p}\eta'$ and $p\bar{p}\omega$ decays with various hadronic form factors. In general, the main purpose of this paper is to emphasize the importance of the contribution of the nucleon-pole diagram in studying N^*'s via various $J/\psi \to N\bar{N}M$ processes and to provide an indication of how big the deviation would be if the vertex form factors are applied in data analysis.

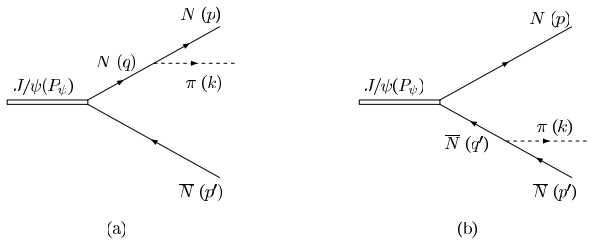

Fig. 3. Nucleon-pole diagrams for the $J/\psi \to \pi N\bar{N}$ decay.

The paper is organized in the following way: in the next section, the nucleon-pole contributions in the $J/\psi \to N\bar{N}\pi$, $p\bar{p}\eta$ and $p\bar{p}\eta'$ decays with and without form factors are systematically studied. The nucleon-pole contribution in the $J/\psi \to N\bar{N}\omega$ decay is demonstrated in sect. 3, and in sect. 4, the conclusions are drawn.

2 Nucleon-pole contributions in the $J/\psi \to N\bar{N}\pi$, $p\bar{p}\eta$ and $p\bar{p}\eta'$ decays

Firstly, we take the $J/\psi \to N\bar{N}\pi$ channel as a sample to analyze cautiously the off-shell effect through different $NN\pi$ couplings and various form factors. And then, we discuss the results in the $J/\psi \to N\bar{N}\eta$ and $N\bar{N}\eta'$ channels.

2.1 Nucleon-pole contributions by using different $NN\pi$ couplings in the $J/\psi \to N\bar{N}\pi$ decay

The nucleon-pole diagrams for $J/\psi \to \pi N\bar{N}$ are shown in fig. 3, with $q = p + k = P_\psi - p'$ and $q' = p' + k = P_\psi - p$. In the case of very low energy of the pion, the dominant contribution to the $J/\psi \to N\bar{N}\pi$ decay comes from the nucleon-pole diagram. However, when the energy of the pion becomes greater, the contribution of the nucleon-pole diagram is evidently greater than in the experimental data. Thus, the off-shell effect of the nucleon propagator should be carefully studied. Generally, the $J/\psi \to N\bar{N}$ interaction can be written as

$$H_\psi = \bar{N}\left[F_M\gamma^\mu + \frac{1}{2m}F_0\left(p - p'\right)^\mu\right] N\ \epsilon_\mu(P_\psi), \qquad (1)$$

where m is the mass of the nucleon, P_ψ, p and p' are the four-momenta of J/ψ, N and $\bar{N}$, respectively, and $\epsilon_\mu(P_\psi)$ denotes the polarization vector of J/ψ. Dimensionless real decay constants F_M and F_0 can be determined by the experimental data of the two-body decay $J/\psi \to p\bar{p}$. There are two forms for pion-nucleon interaction which are widely employed in the literatures. One is in pseudoscalar-pseudoscalar (PS-PS) form:

$$H_1 = ig_{N\bar{N}\pi}\bar{N}\gamma_5\vec{\tau}N\vec{\pi}, \qquad (2)$$

and the other is in pseudoscalar-pseudovector (PS-PV) form:

$$H_1' = \frac{1}{2m}g_{N\bar{N}\pi}\bar{N}\gamma_5\gamma_\mu\vec{\tau}N\partial^\mu\vec{\pi}, \qquad (3)$$

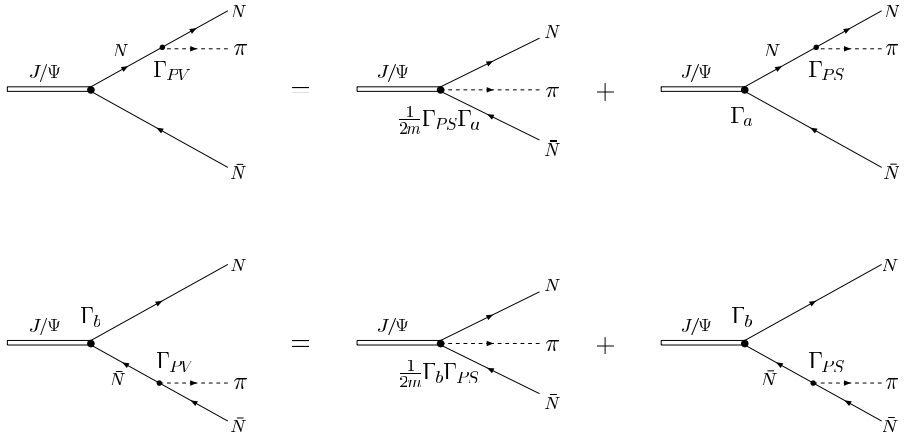

Fig. 4. Diagrammatic expressions of eq. (8) for the upper-row diagrams and of eq. (9) for the lower-row diagrams, respectively.

where $\vec{\tau}$ is the isospin Pauli matrix, and $g_{N\bar{N}\pi}$ is the pion-nucleon coupling constant with [7]

$$(g_{N\bar{N}\pi})^2/4\pi \simeq 14.8. \tag{4}$$

When the intermediate nucleon is on-shell, the decay amplitude of fig. 3 in the PS-PS coupling π-N interaction can be derived as

$$\begin{aligned}\mathcal{M}_{\rm PS}^{\rm on} &= ig_{N\bar{N}\pi}\bar{u}(p)\gamma_5\left[F_M\left(\frac{\not{k}\not{\epsilon}}{2p\cdot k+k^2}-\frac{\not{\epsilon}\not{k}}{2p'\cdot k+k^2}\right)\right.\\ &\left.+\frac{F_0}{m}\not{k}\left(\frac{p\cdot\epsilon}{2p'\cdot k+k^2}-\frac{p'\cdot\epsilon}{2p\cdot k+k^2}\right)\right]v(p') \qquad (5)\\ &\equiv \mathcal{M}_{\rm PS}.\end{aligned}$$

It also can easily be proved that the decay amplitude in the PS-PV coupling case takes the same form, namely

$$\mathcal{M}_{\rm PV}^{\rm on} = \mathcal{M}_{\rm PS}. \tag{6}$$

Thus, no matter whether PS-PS coupling or the PS-PV coupling is employed, the yielded decay amplitudes would be exactly the same.

It can further be verified that when the intermediate nucleon is off-shell, the decay amplitude of fig. 3 in the PS-PS coupling case still takes the same form as in the on-shell case:

$$\mathcal{M}_{\rm PS}^{\rm off} = \mathcal{M}_{\rm PS}, \tag{7}$$

but in the PS-PV coupling case, it has additional terms:

$$\begin{aligned}\mathcal{M}_{{\rm PV},a}^{\rm off} &= \frac{ig_{N\bar{N}\pi}}{2m}\bar{u}(p)\gamma_5\\ &\times\left[F_M\gamma^\mu\epsilon_\mu+\frac{1}{2m}F_0(q-p')^\mu\epsilon_\mu\right]v(p')+\mathcal{M}_{{\rm PS},a}\,, \qquad (8)\\ \mathcal{M}_{{\rm PV},b}^{\rm off} &= \frac{ig_{N\bar{N}\pi}}{2m}\bar{u}(p)\\ &\times\left[F_M\gamma^\mu\epsilon_\mu+\frac{1}{2m}F_0(p-q')^\mu\epsilon_\mu\right]\gamma_5 v(p')+\mathcal{M}_{{\rm PS},b}\,, \qquad (9)\end{aligned}$$

and

$$\mathcal{M}_{{\rm PS},a}+\mathcal{M}_{{\rm PS},b} = \mathcal{M}_{\rm PS}, \tag{10}$$

where the subscripts a and b denote the decay amplitudes of fig. 3(a) and fig. 3(b), respectively. Equations (8) and (9) can also be expressed diagrammatically as in fig. 4, where the vertices Γ_a, Γ_b, $\Gamma_{\rm PS}$ and $\Gamma_{\rm PV}$ are $\Gamma_a = F_M\gamma^\mu + \frac{1}{2m}F_0(q-p')^\mu$, $\Gamma_b = F_M\gamma^\mu + \frac{1}{2m}F_0(p-q')^\mu$, $\Gamma_{\rm PS} = ig_{N\bar{N}\pi}\gamma_5$ and $\Gamma_{\rm PV} = \frac{i}{2m}g_{N\bar{N}\pi}\gamma_5\gamma_\mu k^\mu$, respectively. The total decay amplitude for fig. 3 is then obtained by summing over eq. (8) and eq. (9):

$$\begin{aligned}\mathcal{M}_{\rm PV}^{\rm off} &= \mathcal{M}_{{\rm PV},a}^{\rm off}+\mathcal{M}_{{\rm PV},b}^{\rm off}\\ &= \frac{ig_{N\bar{N}\pi}}{2m^2}F_0\bar{u}(p)(p-p')^\mu\epsilon_\mu\gamma_5 v(p')+\mathcal{M}_{\rm PS} \qquad (11)\\ &\equiv \mathcal{M}_{\rm PV}.\end{aligned}$$

It is clear that in the $J/\psi \to N\bar{N}\pi$ process, when the π-N interaction takes the PS-PV coupling form, the decay amplitude would receive not only the same contribution from the PS-PS coupling, but also an extra contribution from the contact term. Moreover, the difference of the decay amplitudes in the PS-PS and PS-PV coupling cases only relates to $|F_0|$, and is more distinct at a large value of $|F_0|$.

The differential decay rate can be formulated by summing over possible spin states of the final nucleon and anti-nucleon:

$$\begin{aligned}{\rm d}\Gamma_{\rm PS}(J/\psi\to N\bar{N}\pi) &= \frac{2\pi^4}{2M_\psi}|\mathcal{M}_{\rm PS}|^2\,{\rm d}\Phi_3(P_\psi;p,p',k)\\ &= (2\pi)^4\frac{2g_{N\bar{N}\pi}^2}{M_\psi}\left[|F_M|^2A_{{\rm PS},1}+|F_0|^2A_{{\rm PS},2}\right.\\ &\left.+{\rm Re}\left(F_0^*F_M\right)A_{{\rm PS},3}\right]{\rm d}\Phi_3(P_\psi;p,p',k), \qquad (12)\end{aligned}$$

$$\begin{aligned}{\rm d}\Gamma_{\rm PV}(J/\psi\to N\bar{N}\pi) &= \frac{2\pi^4}{2M_\psi}|\mathcal{M}_{\rm PV}|^2\,{\rm d}\Phi_3(P_\psi;p,p',k)\\ &= (2\pi)^4\frac{2g_{N\bar{N}\pi}^2}{M_\psi}\left[|F_M|^2A_{{\rm PS},1}+|F_0|^2\left(A_{{\rm PS},2}+A_{{\rm PV},2}\right)\right.\\ &\left.+{\rm Re}\left(F_0^*F_M\right)\left(A_{{\rm PS},3}+A_{{\rm PV},3}\right)\right]{\rm d}\Phi_3(P_\psi;p,p',k), \qquad (13)\end{aligned}$$

with M_ψ being the mass of J/ψ and

$$\mathrm{d}\Phi_3\big(P_\psi;p,p',k\big)=\delta^4\big(P_\psi-p-p'-k\big)\times\frac{\mathrm{d}^3p}{(2\pi)^3 2p_0}\frac{\mathrm{d}^3p'}{(2\pi)^3 2p'_0}\frac{\mathrm{d}^3k}{(2\pi)^3 2k_0} \quad (14)$$

being an element of the three-body phase space. The explicit expressions for $A_{\mathrm{PS},i}(i=1,2,3)$ and $A_{\mathrm{PV},i}(i=2,3)$ are shown in the appendix. Again, it is found from eqs. (12) and (13) that the $|F_M|^2$-dependent term does not contribute to the difference between $\mathrm{d}\Gamma_{\mathrm{PV}}$ and $\mathrm{d}\Gamma_{\mathrm{PS}}$. If $|F_0|=0$, the differential decay rates in the PS-PS and PS-PV coupling cases are absolutely identical.

The value of $|F_0|/|F_M|$ can be determined in the following way [7]. In the realistic calculation, one usually adopts the electric coupling parameter F_E and the magnetic coupling parameter F_M instead of F_0 and F_M used above. F_0 can be expressed by

$$F_0=\frac{4m^2}{M_\psi-4m^2}\big(F_M-F_E\big). \quad (15)$$

Then the squared amplitude for $J/\psi\to p\bar{p}$ decay can be written as

$$\overline{|\mathcal{M}|^2}=C_0\ \big(1+\alpha\cos^2\theta\big), \quad (16)$$

with

$$C_0=m^2|F_M|^2+4m^2|F_E|^2,$$
$$\alpha=\left[|F_M|^2-\frac{4m^2}{M_\psi^2}|F_E|^2\right]\Big/\left[|F_M|^2+\frac{4m^2}{M_\psi^2}|F_E|^2\right]. \quad (17)$$

By measuring the angular distribution of the $J/\psi\to p\bar{p}$ decay, one obtains $\alpha=0.62\pm0.11$ [8]. Consequently, $|F_E|/|F_M|=0.80\pm0.14$. Assuming

$$\frac{F_E}{F_M}=\frac{|F_E|}{|F_M|}\ e^{i\delta}, \quad (18)$$

one can easily extract the value of $|F_0|/|F_M|$ as

$$\frac{F_0}{F_M}=\frac{4m^2}{M_\psi^2-4m^2}\left[1-\frac{|F_E|}{|F_M|}\ e^{i\delta}\right]. \quad (19)$$

Taking $\delta=0$, $\frac{\pi}{2}$ and π, we have

$$\frac{|F_0|}{|F_M|}=\begin{cases}0.12\pm0.08 & \text{for } \delta=0,\\ 0.74\pm0.08 & \text{for } \delta=\dfrac{\pi}{2},\\ 1.04\pm0.08 & \text{for } \delta=\pi.\end{cases} \quad (20)$$

The effect of the ratio $|F_0|/|F_M|$ on Γ_{PS} and Γ_{PV} can be shown by taking $|F_0|/|F_M|=0,0.12,0.74,1.04$ in our calculation. The branching ratios (BR) of the decay widths for fig. 3 in the PS-PS and PS-PV cases are[1]

$$\frac{\Gamma_{\mathrm{PS}}\big(J/\psi\to p\bar{p}\pi^0\big)}{\Gamma(J/\psi\to p\bar{p})}=\begin{cases}0.556 & \text{for } |F_0|/|F_M|=0,\\ 0.561 & \text{for } |F_0|/|F_M|=0.12,\\ 0.688 & \text{for } |F_0|/|F_M|=0.74,\\ 0.815 & \text{for } |F_0|/|F_M|=1.04,\end{cases} \quad (21)$$

and

$$\frac{\Gamma_{\mathrm{PV}}\big(J/\psi\to p\bar{p}\pi^0\big)}{\Gamma(J/\psi\to p\bar{p})}=\begin{cases}0.556 & \text{for } |F_0|/|F_M|=0,\\ 0.529 & \text{for } |F_0|/|F_M|=0.12,\\ 0.475 & \text{for } |F_0|/|F_M|=0.74,\\ 0.421 & \text{for } |F_0|/|F_M|=1.04,\end{cases} \quad (22)$$

respectively. Comparing with the empirical ratio [9]

$$\frac{\Gamma\big(J/\psi\to p\bar{p}\pi^0\big)}{\Gamma(J/\psi\to p\bar{p})}=0.51\pm0.04, \quad (23)$$

one can see that the resultant BRs in eqs. (21) and (22) are very close to the data values. This indicates that the BR of the $J/\psi\to N\bar{N}\pi$ decay is dominated by the nucleon-pole diagrams of fig. 3 without including the hadronic form factor. Of course, the N^*-pole will also contribute. However, if one used the data of $J/\psi\to N\bar{N}\pi$ decay to study N^*, one could not get meaningful information until the nucleon-pole contribution is considered.

One can also find that the difference due to different πN couplings becomes larger when the $|F_0|/|F_M|$ ratio increases. This is because in the PS-PS coupling case, both the F_M-dependent and the F_0-dependent term contribute positively, but in the PS-PV coupling case, the F_M-dependent term keeps the same contribution and the F_0-dependent term gives a negative contribution. Therefore, a large $|F_0|/|F_M|$ value would make the difference larger. For instance, with $|F_0|/|F_M|=1.04$, the ratio $\Gamma_{\mathrm{PS}}(J/\psi\to p\bar{p}\pi^0)/\Gamma(J/\psi\to p\bar{p})$ is almost twice the ratio $\Gamma_{\mathrm{PV}}(J/\psi\to p\bar{p}\pi^0)/\Gamma(J/\psi\to p\bar{p})$.

2.2 Off-shell effects with various form factors in the $J/\psi\to N\bar{N}\pi$ decay

Normally, a hadronic form factor is applied to the meson-baryon-baryon (MBB') vertices because of the inner quark-gluon structure of hadrons. It is well known that form factors play an important role in many physics processes, for example, the N-N interaction models [10], NN scattering [11], πN scattering [12–14], pion photoproduction [15], vector meson photoproduction [16], etc. However, due to the difficulties in dealing with non-perturbative QCD (NPQCD) effects, the form factors are commonly adopted phenomenologically.

The most commonly used form factors for meson-nucleon-nucleon vertices are the monopole form factor and the dipole form factor [17]:

$$F_1\big(q^2\big)=\frac{\Lambda^2+m^2}{\Lambda^2+q^2}\,, \quad (24)$$

$$F_2\big(q^2\big)=\frac{\Lambda^4+m^4}{\Lambda^4+q^4}\,, \quad (25)$$

where m and q are the mass and the four-momentum of the intermediate particle, respectively, and Λ is the so-called cut-off momentum that can be determined by fitting the experimental data. The monopole form factor is mainly

[1] The corresponding ratios in ref. [7] are larger than ours due to their large deviation in the phase space integration.

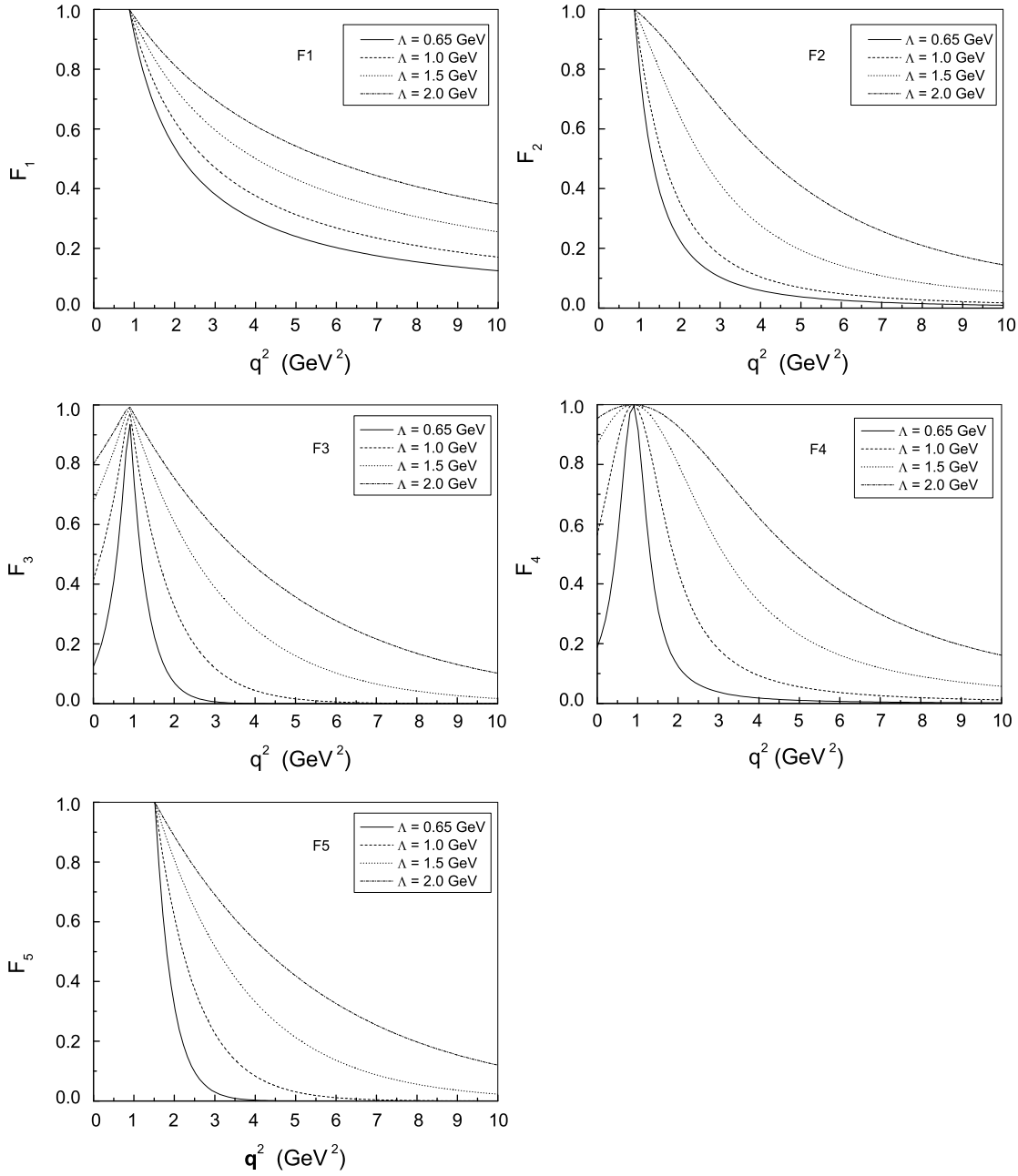

Fig. 5. The momentum-dependence of form factors F_1–F_5 with different Λ values.

used in the π-N and N-N interactions, while the dipole one is usually applied to the N-N interaction. The values of Λ are different process by process. A typical value of Λ for a monopole form factor in the Bonn potential is in the region of 1.3–2 GeV [10], and for the π-N interaction is about 1.35 GeV. Frankfurt and Strikman [18] analyzed the deep inelastic scattering (DIS) of leptons from nucleons and showed that the DIS data support a πNN monopole form factor with $\Lambda \leq 650\,\mathrm{MeV}$.

The exponential form factor is also a frequently used meson-nucleon-nucleon form factor [19],

$$F_3(q^2) = e^{-|q^2-m^2|/\Lambda^2}. \tag{26}$$

The form factor can also take the following form [20,21]:

$$F_4(q^2) = \frac{1}{1+(q^2-m^2)^2/\Lambda^4}\,. \tag{27}$$

Moreover, in the study of meson photoproduction, T.-S.H. Lee *et al.* [21,22] chose a form factor with the following form:

$$F_5(\mathbf{q}^2) = \exp\left[-(\mathbf{q}^2-\mathbf{q}_0^2)/\Lambda^2\right], \tag{28}$$

where $\mathbf{q}$ and $\mathbf{q}_0$ are the three-momentum vectors of the intermediate nucleon at the energy $\sqrt{s}$ ($s=q^2$) and at the nucleon-pole position, respectively.

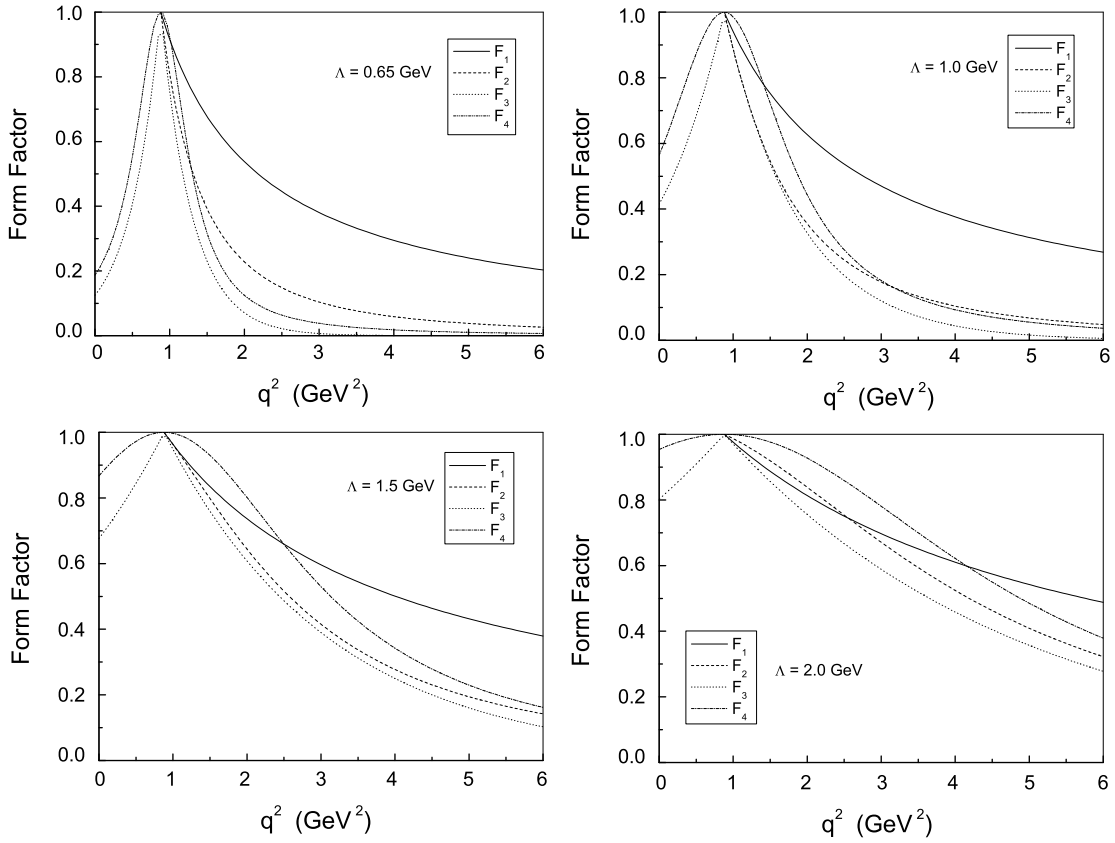

Fig. 6. The momentum-dependence of form factors F_1–F_4 with the same value of Λ.

It should be mentioned that all the form factors mentioned above are normalized to unity when the intermediate nucleon is on its mass shell.

To give the readers a comprehensive idea of various form factors, we plot them with $\Lambda = 0.65$, 1.0, 1.5 and 2.0 GeV in figs. 5 and 6, respectively. Figure 5 shows the Λ-dependence of the form factors given above. The common feature of these form factors is that their high-momentum-transfer part is even more reduced when the Λ value becomes smaller. The momentum-dependent behaviors of these form factors are quite different with different Λ values. Figure 6 presents the momentum-dependence of various form factors. The momentum-dependence of form factors F_2, F_3 and F_4 is very sensitive to the Λ value, but that of F_1 is not. When the value of Λ becomes smaller, the difference among the various form factors is more pronounced. For instance, when $\Lambda = 0.65$ GeV, with increasing q^2, F_3 reduces much more than F_1 does. Since in the decay processes considered in this paper, the intermediate nucleon is off-shell, introducing an off-shell form factor would suppress the off-shell effect of the nucleon, and the form of the form factor and the value of Λ would affect the decay amplitude. Therefore, studying the hadronic vertex form factor can provide a constraint to the data analysis. Moreover, the results of the data fitting can also help us to choose a proper form factor for the $J/\psi \to N\bar{N}M$ investigation.

Suppose that form factors with same form are applied on both vertices of the considered decay diagram, respectively. After adding the form factors, eqs. (6), (7) and (12) can be re-written as

$$\begin{aligned}\mathcal{M}'_{\rm PS} = & ig_{N\bar{N}\pi}\bar{u}(p)\gamma_5 \\ & \times\left[F_M\left(\frac{\not{k}\not{\epsilon}}{2p\cdot k+k^2}F^2(q^2)-\frac{\not{\epsilon}\not{k}}{2p'\cdot k+k^2}F^2(q'^2)\right)\right. \\ & +\frac{F_0}{m}\not{k}\left(\frac{p\cdot\epsilon}{2p'\cdot k+k^2}F^2(q'^2)\right. \\ & \left.\left.-\frac{p'\cdot\epsilon}{2p\cdot k+k^2}F^2(q^2)\right)\right]v(p'), \end{aligned} \tag{29}$$

and

$$\begin{aligned}\mathcal{M}'_{\rm PV} = & \frac{ig_{N\bar{N}\pi}}{2m}\bar{u}(p)\left\{F_M\left[F^2(q^2)-F^2(q'^2)\right]\not{\epsilon}+\frac{F_0}{m}\right. \\ & \left.\times\left[F^2(q'^2)(p\cdot\epsilon)-F^2(q^2)(p'\cdot\epsilon)\right]\right\}\gamma_5 v(p')+\mathcal{M}'_{\rm PS}, \end{aligned} \tag{30}$$

respectively. The form factor $F(q^2)$ can be chosen to be of one of the forms given in eqs. (24)-(28).

In order to show how sensitive the decay BR is to the form of the form factor and to the value of Λ, we take $\Lambda =$ 0.65, 1.0, 1.5 and 2.0 GeV and $|F_0|/|F_M| = 0.12 \pm 0.08$, and calculate the BR $\Gamma(J/\psi \to p\bar{p}\pi^0)/\Gamma(J/\psi \to p\bar{p})$ with all kinds of form factors shown above. The results

Table 1. The BR $\Gamma(J/\psi \to p\bar{p}\pi^0)/\Gamma(J/\psi \to p\bar{p})$ (%) with various form factors.

F.F.	πN coupling	$\Lambda = 0.65\,\mathrm{GeV}$	$\Lambda = 1.0\,\mathrm{GeV}$	$\Lambda = 1.5\,\mathrm{GeV}$	$\Lambda = 2.0\,\mathrm{GeV}$
F_1	PS	3.95(3.73–4.18)	6.81(6.45–7.20)	12.69(12.05–13.38)	19.35(18.40–20.37)
	PV	2.79(2.77–2.82)	5.04(5.01–5.07)	9.96(9.91–9.98)	15.89(15.83–15.91)
F_2	PS	0.34(0.32–0.37)	1.23(1.15–1.31)	7.21(6.82–7.64)	19.64(18.66–20.71)
	PV	0.20(0.19–0.21)	0.76(0.75–0.78)	5.07(5.02–5.11)	15.50(15.45–15.53)
F_3	PS	0.07(0.06–0.07)	1.09(1.02–1.16)	5.83(5.51–6.18)	13.29(12.61–14.02)
	PV	0.04(0.03–0.04)	0.66(0.64–0.68)	4.07(4.03–4.10)	10.23(10.18–10.25)
F_4	PS	0.23(0.22–0.25)	3.35(3.15–3.58)	15.03(14.23–15.89)	29.70(29.68–31.26)
	PV	0.13(0.12–0.13)	2.08(2.04–2.14)	10.98(10.92–11.04)	24.30(24.23–24.31)
F_5	PS	2.39(2.25–2.54)	10.25(9.71–10.83)	23.91(22.75–25.16)	34.01(32.40–35.72)
	PV	2.33(2.16–2.81)	9.28(9.37–9.33)	21.98(22.12–21.85)	31.57(31.63–31.44)

are tabulated in table 1, where the numbers in parentheses correspond to the lower and the upper limits of $|F_0|/|F_M|$, respectively. From table 1, one can see that no matter which form factor is employed, the difference between $\Gamma_{\mathrm{PV}}(J/\psi \to p\bar{p}\pi^0)$ and $\Gamma_{\mathrm{PS}}(J/\psi \to p\bar{p}\pi^0)$ is generally larger than that in the case without form factor. For instance, when $\Lambda = 1.0\,\mathrm{GeV}$,

$$\frac{\Gamma_{\mathrm{PV}}\big(J/\psi \to p\bar{p}\pi^0\big)}{\Gamma_{\mathrm{PS}}(J/\psi \to p\bar{p}\pi^0)} = \begin{cases} 0.74 & \text{for } F_1, \\ 0.618 & \text{for } F_2, \\ 0.606 & \text{for } F_3, \\ 0.621 & \text{for } F_4, \\ 0.905 & \text{for } F_5, \end{cases} \tag{31}$$

and the corresponding ratio without form factors is

$$\frac{\Gamma_{\mathrm{PV}}\big(J/\psi \to p\bar{p}\pi^0\big)}{\Gamma_{\mathrm{PS}}(J/\psi \to p\bar{p}\pi^0)} \simeq 0.940. \tag{32}$$

It means that the introduced form factor suppresses the contribution in the large-momentum-transfer region, and consequently, enlarges the off-shell effects in the PS-PS and PS-PV coupling cases to a different extent. For a specific form factor, when the Λ value reduces, the curve of the form factor bends towards the lower momentum direction. It further suppresses the contribution in the high-momentum-transfer region, enlarges the off-shell effect and reduces the nucleon-pole contribution. For instance, with form factor F_5, when Λ reduces from 2.0 GeV to 0.65 GeV, the BR $\frac{\Gamma_{\mathrm{PV}}(J/\psi \to p\bar{p}\pi^0)}{\Gamma(J/\psi \to p\bar{p})}$ decreases from 31.57% to 2.33%. The Λ-dependence of the BR differs in the different form factor cases. For the same amount of Λ value change, the BR with F_1 decreases by about 1/5, but the BR with F_3 drops to about 1/256. The BR with a larger Λ value is more pronounced, and the nucleon-pole contribution is important. On the contrary, the nucleon-pole contribution by using a small Λ value can be ignored.

The BRs with different form factors but the same Λ value are quite different. For example, when $\Lambda = 0.65\,\mathrm{GeV}$, the BRs with F_3 and F_1 in the PS-PV coupling case are about 0.04% and 2.79%, respectively. The latter is about 70 times larger than the former one. Anyway, these BRs are negligibly smaller than the data value of 51%. However, when Λ is large, the difference between different form factor cases becomes very small; consequently, the contribution from the high-momentum part is not much suppressed, the resultant BRs in both PS-PS and PS-PV cases are close to each other and are comparable with the data. For instance, when $\Lambda = 2.0\,\mathrm{GeV}$, the maximum range of the BR change is from 10.23% to 34.01%.

Since it is not sure which form factor is suitable for the considered decay processes, we cannot conclude whether the nucleon pole is dominantly responsible for the BR of the $J/\psi \to N\bar{N}\pi$ decay. Now, we would show how much the nucleon-pole diagram contributes to the BR of $J/\psi \to N\bar{N}\pi$ decay, when a form factor used in a similar process is adopted. It should be mentioned that although all the form factors shown above are the $NN\pi$ vertex form factors, the particle which the momentum variable corresponds to is different case by case. In the N-N interaction, the form factor is π-momentum dependent, and in the π-N interaction, in the pion photoproduction, and in the $J/\psi \to N\bar{N}\pi$ decay, it is intermediate–nucleon-momentum dependent. Only in the case in which the form factor depends on the four-momenta of the three interacting particles [12], a unified form factor with the same proper parameter Λ can possibly be applied to all mentioned processes. We summarize in table 2 part of form factors whose momentum dependence is similar with respect to the $J/\psi \to N\bar{N}\pi$ decay and whose Λ value has well been determined by the πN scattering or by the pion photoproduction

With these form factors, we re-calculate the BR $\Gamma(J/\psi \to p\bar{p}\pi^0)/\Gamma(J/\psi \to p\bar{p})$. The resultant BRs with $|F_0|/|F_M| = 0.12$ are

$$\frac{\Gamma\big(J/\psi \to p\bar{p}\pi^0\big)}{\Gamma(J/\psi \to p\bar{p})} = \begin{cases} 0.0808 & \text{for } F_1, \\ 0.0465 & \text{for } F_4, \\ 0.0967 & \text{for } F_5. \end{cases} \tag{33}$$

Table 2. πNN form factors frequently used in the literatures.

πN Coupling	Coupling Constant	F.F.	Λ (cut-off)	Reference
PV	$f^2_{\pi NN}/4\pi = 0.0778$	$F_1(q^2)$	1350 MeV	[14]
PV	$g^2_{\pi NN}/4\pi = 14.3$	$F_4(q^2)$	1116.6 MeV	[13]
PV	$f^2_{\pi NN}/4\pi = 0.0778$	$F_4(q^2)$	1200 MeV	[14]
PS	$g^2_{\pi NN}/4\pi = 14$	$F_5(q^2)$	1000 MeV	[21]

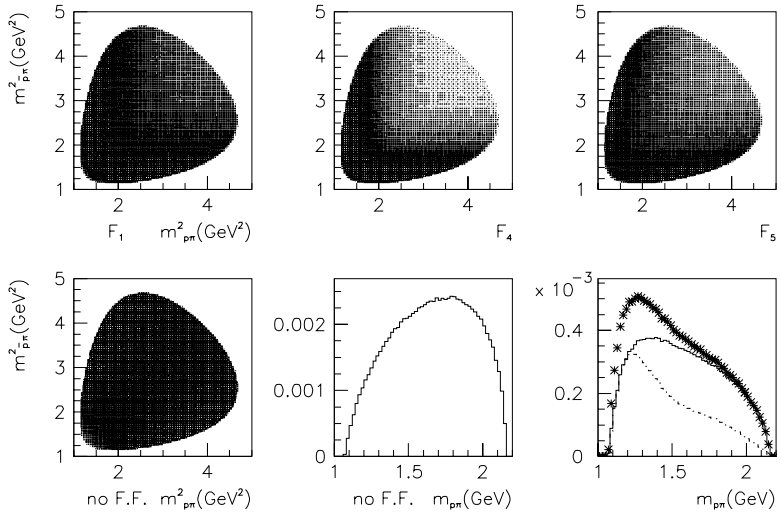

Fig. 7. The Dalitz plot and the invariant $p\pi^0$ mass distribution of the $J/\psi \to p\bar{p}\pi^0$ decay with the form factors F_1, F_4, and F_5. The solid curve, the dot-dashed curve and the starred curve in the invariant-mass distribution figure correspond to the form factors F_1, F_4, and F_5, respectively.

And those with $|F_0|/|F_M| = 1.04$ are

$$\frac{\Gamma\left(J/\psi \to p\bar{p}\pi^0\right)}{\Gamma(J/\psi \to p\bar{p})} = \begin{cases} 0.0735 & \text{for } F_1, \\ 0.0524 & \text{for } F_4, \\ 0.1636 & \text{for } F_5. \end{cases} \tag{34}$$

Comparing with the results in table 1, one finds that the resultant BRs do not differ as much as those in table 1, but there is still visible difference.

Although the magnitude of the BR is much smaller than the data values, it can still be used to select a proper form factor for the $J/\psi \to N\bar{N}\pi$ decay. To fulfil this goal, in terms of a Monte Carlo simulation, we calculate the Dalitz plot and the invariant $p\pi^0$ mass distribution of the $J/\psi \to p\bar{p}\pi^0$ decay with the form factors F_1, F_4, and F_5, respectively. They are shown in fig. 7. Comparing these figures with the data, one should be able to find out the most suitable form factor for the $J/\psi \to p\bar{p}\pi^0$ decay.

2.3 Nucleon-pole contributions in the $J/\psi \to p\bar{p}\eta$ and $J/\psi \to p\bar{p}\eta'$ decays

The corresponding Feynman diagrams for the $J/\psi \to p\bar{p}\eta$ and $p\bar{p}\eta'$ decays are shown in fig. 8. The same formulae for the $J/\psi \to p\bar{p}\pi^0$ decay can be applied to the $J/\psi \to p\bar{p}\eta$ and $J/\psi \to p\bar{p}\eta'$ decays, but replacing $g_{N\bar{N}\pi}$ with $g_{N\bar{N}\eta}$ or $g_{N\bar{N}\eta'}$, because π, η and η' are all pseudoscalar mesons. The values of $g_{N\bar{N}\eta}$ and $g_{N\bar{N}\eta'}$ can be chosen according to the following relations [7]:

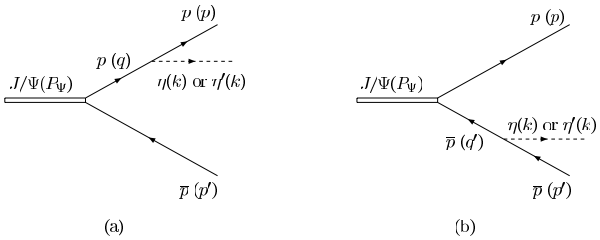

Fig. 8. Proton-pole diagrams for $J/\psi \to p\bar{p}\eta$ and $J/\psi \to p\bar{p}\eta'$ decays.

$$\begin{aligned} \left(g_{\eta NN}/g_{\pi NN}\right)^2 &= 3.90625 \times 10^{-3}, \\ \left(g_{\eta' NN}/g_{\pi NN}\right)^2 &= 2.5 \times 10^{-3}. \end{aligned} \tag{35}$$

And we take $|F_0|/|F_M| = 0, 0.12, 0.74$ and 1.04 in our calculation. The decay ratios $\Gamma(J/\psi \to p\bar{p}\eta)/\Gamma(J/\psi \to p\bar{p})$ and $\Gamma(J/\psi \to p\bar{p}\eta')/\Gamma(J/\psi \to p\bar{p})$ from the proton-pole contribution without considering

Table 3. Branching ratio $\Gamma(J/\psi \to p\bar{p}\eta)/\Gamma(J/\psi \to p\bar{p})$ with form factors, with $|F_0|/|F_M| = 0.12$.

F.F.	$\pi\eta$ coupling	$\Lambda = 0.65\,\mathrm{GeV}$	$\Lambda = 1.0\,\mathrm{GeV}$	$\Lambda = 1.5\,\mathrm{GeV}$	$\Lambda = 2.0\,\mathrm{GeV}$
F_1	PS	9.61×10^{-6}	2.24×10^{-5}	5.92×10^{-5}	1.14×10^{-4}
	PV	7.26×10^{-6}	1.74×10^{-5}	4.77×10^{-5}	9.49×10^{-5}
F_2	PS	6.34×10^{-8}	5.04×10^{-7}	1.31×10^{-5}	8.90×10^{-5}
	PV	4.15×10^{-8}	3.35×10^{-7}	9.26×10^{-6}	6.91×10^{-5}
F_3	PS	2.63×10^{-11}	1.54×10^{-7}	1.00×10^{-5}	5.31×10^{-5}
	PV	1.63×10^{-11}	1.01×10^{-7}	7.02×10^{-6}	4.09×10^{-5}
F_4	PS	1.77×10^{-9}	6.77×10^{-7}	3.40×10^{-5}	1.63×10^{-4}
	PV	1.11×10^{-9}	4.37×10^{-7}	2.39×10^{-5}	1.29×10^{-4}
F_5	PS	7.06×10^{-7}	2.64×10^{-5}	1.38×10^{-4}	2.52×10^{-4}
	PV	3.66×10^{-6}	2.19×10^{-5}	1.22×10^{-4}	2.29×10^{-4}

Table 4. Branching ratio $\Gamma(J/\psi \to p\bar{p}\eta')/\Gamma(J/\psi \to p\bar{p})$ with form factors, with $|F_0|/|F_M| = 0.12$.

F.F.	$\pi\eta'$ coupling	$\Lambda = 0.65\,\mathrm{GeV}$	$\Lambda = 1.0\,\mathrm{GeV}$	$\Lambda = 1.5\,\mathrm{GeV}$	$\Lambda = 2.0\,\mathrm{GeV}$
F_1	PS	1.35×10^{-7}	3.61×10^{-7}	1.16×10^{-6}	2.59×10^{-6}
	PV	1.14×10^{-7}	3.09×10^{-7}	1.01×10^{-6}	2.28×10^{-6}
F_2	PS	1.99×10^{-10}	1.96×10^{-9}	9.94×10^{-8}	1.33×10^{-6}
	PV	1.53×10^{-10}	1.52×10^{-9}	7.93×10^{-8}	1.11×10^{-6}
F_3	PS	4.78×10^{-18}	5.99×10^{-11}	6.40×10^{-8}	7.76×10^{-7}
	PV	3.62×10^{-18}	4.16×10^{-11}	4.99×10^{-8}	6.50×10^{-7}
F_4	PS	1.70×10^{-12}	1.22×10^{-9}	2.28×10^{-7}	2.63×10^{-6}
	PV	1.26×10^{-12}	9.15×10^{-10}	1.79×10^{-7}	2.21×10^{-6}
F_5	PS	8.13×10^{-10}	2.67×10^{-7}	2.91×10^{-6}	6.75×10^{-6}
	PV	1.23×10^{-7}	2.32×10^{-7}	2.50×10^{-6}	6.05×10^{-6}

form factors are

$$\frac{\Gamma_{\mathrm{PS}}(J/\psi \to p\bar{p}\eta)}{\Gamma(J/\psi \to p\bar{p})} = \begin{cases} 5.48 \times 10^{-4} & \text{for } |F_0|/|F_M| = 0, \\ 5.63 \times 10^{-4} & \text{for } |F_0|/|F_M| = 0.12, \\ 6.91 \times 10^{-4} & \text{for } |F_0|/|F_M| = 0.74, \\ 8.19 \times 10^{-4} & \text{for } |F_0|/|F_M| = 1.04, \end{cases} \tag{36}$$

$$\frac{\Gamma_{\mathrm{PV}}(J/\psi \to p\bar{p}\eta)}{\Gamma(J/\psi \to p\bar{p})} = \begin{cases} 5.48 \times 10^{-4} & \text{for } |F_0|/|F_M| = 0, \\ 5.26 \times 10^{-4} & \text{for } |F_0|/|F_M| = 0.12, \\ 4.69 \times 10^{-4} & \text{for } |F_0|/|F_M| = 0.74, \\ 4.12 \times 10^{-4} & \text{for } |F_0|/|F_M| = 1.04, \end{cases} \tag{37}$$

and

$$\frac{\Gamma_{\mathrm{PS}}(J/\psi \to p\bar{p}\eta')}{\Gamma(J/\psi \to p\bar{p})} = \begin{cases} 1.93 \times 10^{-5} & \text{for } |F_0|/|F_M| = 0, \\ 1.99 \times 10^{-5} & \text{for } |F_0|/|F_M| = 0.12, \\ 2.45 \times 10^{-5} & \text{for } |F_0|/|F_M| = 0.74, \\ 2.91 \times 10^{-5} & \text{for } |F_0|/|F_M| = 1.04, \end{cases} \tag{38}$$

$$\frac{\Gamma_{\mathrm{PV}}(J/\psi \to p\bar{p}\eta')}{\Gamma(J/\psi \to p\bar{p})} = \begin{cases} 1.93 \times 10^{-5} & \text{for } |F_0|/|F_M| = 0, \\ 1.87 \times 10^{-5} & \text{for } |F_0|/|F_M| = 0.12, \\ 1.70 \times 10^{-5} & \text{for } |F_0|/|F_M| = 0.74, \\ 1.54 \times 10^{-5} & \text{for } |F_0|/|F_M| = 1.04. \end{cases} \tag{39}$$

Again, the difference of the BRs between PS-PS and PS-PV couplings decreases when the ratio $|F_0|/|F_M|$ decreases. Comparing with the empirical data $\Gamma(J/\psi \to p\bar{p}\eta)/\Gamma(J/\psi \to p\bar{p}) = 0.98 \pm 0.09$ and $\Gamma(J/\psi \to p\bar{p}\eta')/\Gamma(J/\psi \to p\bar{p}) = 0.42 \pm 0.19$ [9], one finds that the calculated BRs are all smaller by 0.1% with respect to the data. This is because in these two decays, the intermediate nucleon is largely off-shell. We also tabulate the BRs $\frac{\Gamma(J/\psi \to p\bar{p}\eta)}{\Gamma(J/\psi \to p\bar{p})}$ and $\frac{\Gamma(J/\psi \to p\bar{p}\eta')}{\Gamma(J/\psi \to p\bar{p})}$ with various πNN form factors in tables 3 and 4, respectively. Because the form factor further reduces the proton-pole contribution in the high-momentum region, the resultant BRs are very small. Therefore, in analyzing the $J/\psi \to p\bar{p}\eta$ and $J/\psi \to p\bar{p}\eta'$ data, the proton-pole contribution can safely be ignored. The main contributor for such decays must be some other diagrams, for instance, the N^*-pole diagram.

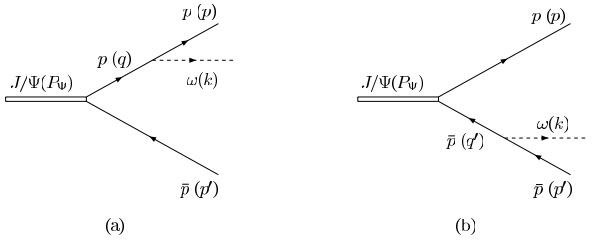

Fig. 9. Proton-pole diagram for the $J/\psi \to p\bar{p}\omega$ decay.

3 Nucleon-pole contribution in the $J/\psi \to p\bar{p}\omega$ decay

The nucleon-pole diagram in the $J/\psi \to p\bar{p}\omega$ decay is shown in fig. 9, where the variables in brackets are the four-momenta of the corresponding particles. The mass of the ω-meson is 781.94 MeV. Due to the heavy mass of ω, the intermediate nucleon in fig. 9 must be far from the mass shell.

The ωNN interaction can be written as [7]

$$H_{\omega NN} = g_{\omega NN}\bar{N}(x)\gamma^{\alpha}N(x)\omega_{\alpha}(x) + i\frac{1}{4m}f_{\omega NN}\bar{N}(x)\big[\gamma^{\mu},\gamma^{\nu}\big]N(x)\partial_{\mu}\omega_{\nu}(x). \quad (40)$$

The vector coupling constant $g_{\omega NN}$ and tensor coupling constant $f_{\omega NN}$ are

$$g^2_{\omega pp}/4\pi \simeq 6.3, \quad (41)$$

$$f_{\omega pp} = \big(\mu_p + \mu_n\big)g_{\omega pp}\,, \quad (42)$$

respectively, with the following anomalous magnetic moments of proton and neutron:

$$\mu_p = 1.7928\mu_N, \qquad \mu_n = -1.9131\mu_N. \quad (43)$$

A simple manipulation gives

$$f_{\omega pp} \simeq -0.12 g_{\omega pp}\,. \quad (44)$$

Therefore, the ωNN interaction is mainly a vector coupling.

Similar to what Y. Oh and T.-S.H. Lee did [15,23] in the vector meson photoproduction study, we only take the vector coupling in the $J/\psi \to p\bar{p}\omega$ calculation

$$H'_{\omega NN} = g_{\omega NN}\bar{N}(x)\gamma^{\alpha}N(x)\omega_{\alpha}(x). \quad (45)$$

Performing a similar derivation in the $J/\psi \to p\bar{p}\pi^0$ case and using the properties

$$P^{\beta}_{\psi}\epsilon_{\beta}\big(P_{\psi},\lambda\big) = 0, \qquad k^{\alpha}e_{\alpha}\big(k,\lambda'\big) = 0, \quad (46)$$

where $\epsilon_{\beta}(P_{\psi},\lambda)$ and $e_{\alpha}(k,\lambda')$ are polarization vectors of J/ψ and ω, respectively, we get the total decay amplitude for fig. 9:

$$\mathcal{M} = g_{\omega pp}\ \bar{u}(p,s)\left\{F_M\left[\frac{2p\cdot e + \not{\epsilon}\not{k}}{2p\cdot k + k^2}\not{\epsilon} - \not{\epsilon}\frac{2p'\cdot e + \not{k}\not{\epsilon}}{2p'\cdot k + k^2}\right] - \frac{F_0}{m}\left[(p'\cdot\epsilon)\frac{2p\cdot e + \not{\epsilon}\not{k}}{2p\cdot k + k^2} + (p\cdot\epsilon)\frac{2p'\cdot e + \not{k}\not{\epsilon}}{2p'\cdot k + k^2}\right]\right\} v\big(p',s'\big), \quad (47)$$

Table 5. The branching ratio $\Gamma(J/\psi \to p\bar{p}\omega)/\Gamma(J/\psi \to p\bar{p})$ with form factor.

F.F.	$\Lambda = 0.65\,\mathrm{GeV}$	$\Lambda = 1.0\,\mathrm{GeV}$	$\Lambda = 1.5\,\mathrm{GeV}$	$\Lambda = 2.0\,\mathrm{GeV}$
F_1	1.48×10^{-3}	3.83×10^{-3}	1.16×10^{-2}	2.49×10^{-2}
F_2	3.34×10^{-6}	3.15×10^{-5}	1.35×10^{-3}	1.48×10^{-2}
F_3	5.03×10^{-12}	2.45×10^{-6}	9.40×10^{-4}	8.66×10^{-3}
F_4	3.83×10^{-8}	2.43×10^{-5}	3.27×10^{-3}	2.88×10^{-2}
F_5	2.02×10^{-5}	3.28×10^{-3}	2.86×10^{-2}	6.18×10^{-2}

and the differential decay width by summing over possible spin states of the initial and final particles

$$\mathrm{d}\Gamma(J/\psi \to p\bar{p}\omega) = \frac{2\pi^4}{2M_{\psi}}\ \overline{|\mathcal{M}|^2}\ \mathrm{d}\Phi_3\big(P_{\psi};p,p',k\big). \quad (48)$$

Taking $|F_0|/|F_M| = 0$, 0.12, 0.74 and 1.04, we obtain the branching ratio

$$\frac{\Gamma(J/\psi \to p\bar{p}\omega)}{\Gamma(J/\psi \to p\bar{p})} = \begin{cases} 0.169 & \text{for } |F_0|/|F_M| = 0, \\ 0.168 & \text{for } |F_0|/|F_M| = 0.12, \\ 0.171 & \text{for } |F_0|/|F_M| = 0.74, \\ 0.175 & \text{for } |F_0|/|F_M| = 1.04. \end{cases} \quad (49)$$

In comparison with the data 0.61 ± 0.12 of [9] one can see that without considering form factors, the proton-pole diagram provides a rather important contribution to the width of the $J/\psi \to p\bar{p}\omega$ decay. As mentioned above, because ω is relatively heavy, the intermediate proton should be far from mass shell, the terms with high power of momentum in the amplitude make the amplitude-*vs.*-momentum curve bend upward and diverge from the normal Breit-Wigner form. This non-physical feature of the amplitude in the high-momentum region should be suppressed by adding off-shell form factors.

After including the form factor, the decay amplitude becomes

$$\mathcal{M}' = g_{\omega pp}\ \bar{u}(p,s)\left\{F_M\left[\frac{2p\cdot e + \not{\epsilon}\not{k}}{2p\cdot k + k^2}\ F^2\big(q^2\big)\not{\epsilon} - \not{\epsilon}\frac{2p'\cdot e + \not{k}\not{\epsilon}}{2p'\cdot k + k^2}\ F^2\big(q'^2\big)\right] - \frac{F_0}{m}\left[(p'\cdot\epsilon)\ \frac{2p\cdot e + \not{\epsilon}\not{k}}{2p\cdot k + k^2}\ F^2\big(q^2\big) + (p\cdot\epsilon)\ \frac{2p'\cdot e + \not{k}\not{\epsilon}}{2p'\cdot k + k^2}\ F^2\big(q'^2\big)\right]\right\} v\big(p',s'\big), \quad (50)$$

where the form factor $F(q^2)$ can be any one of those given in eqs. (24)-(28). Taking $|F_0|/|F_M| = 0.12$ again, we obtain the BRs $\Gamma(J/\psi \to p\bar{p}\omega)/\Gamma(J/\psi \to p\bar{p})$. They are tabulated in table 5. From this table, one finds that the proton-pole contribution is sensitive to the form of the form factor and to the value of Λ.

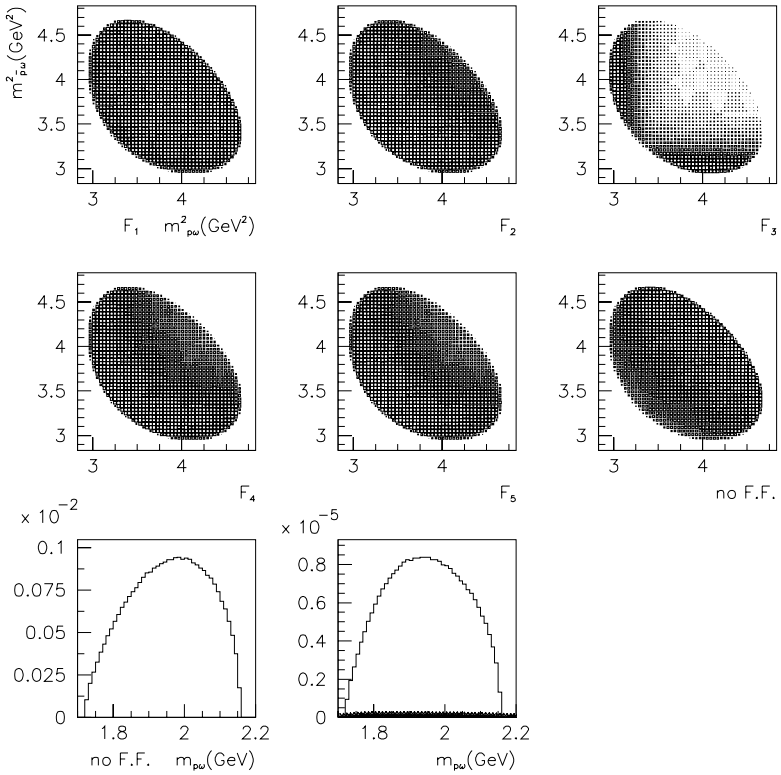

Fig. 10. The Dalitz plot and the $p\omega$ invariant-mass distribution in $J/\psi \to p\bar{p}\omega$ decay ($\Lambda = 0.65\,\mathrm{GeV}$). The solid, dashed, dotted, dot-dashed and starred curves denote the cases with F_1, F_2, F_3, F_4 and F_5, respectively.

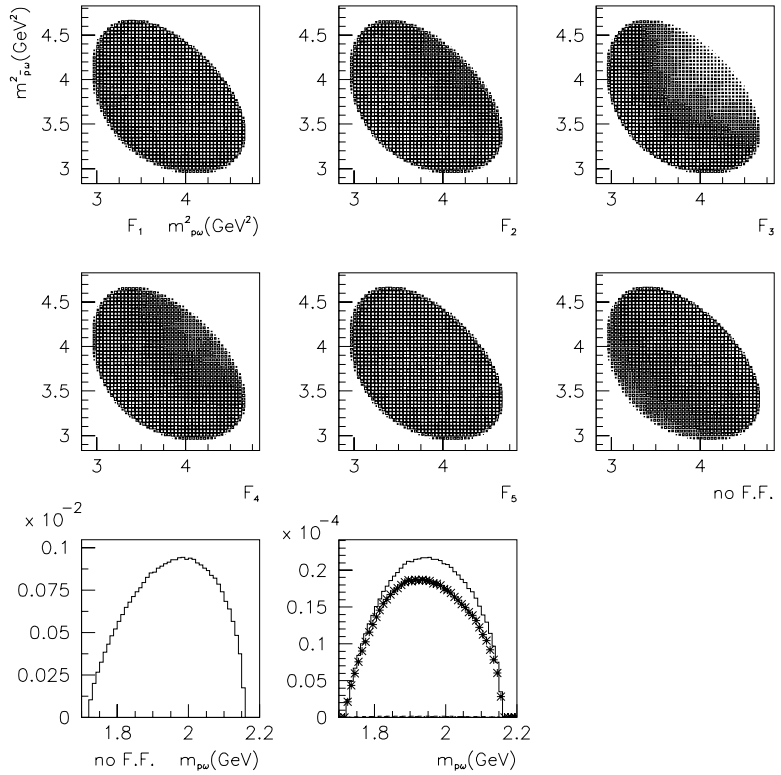

Fig. 11. The Dalitz plot and the $p\omega$ invariant-mass distribution in $J/\psi \to p\bar{p}\omega$ decay ($\Lambda = 1.0\,\mathrm{GeV}$). The solid, dashed, dotted, dot-dashed and starred curves denote the cases with F_1, F_2, F_3, F_4 and F_5, respectively.

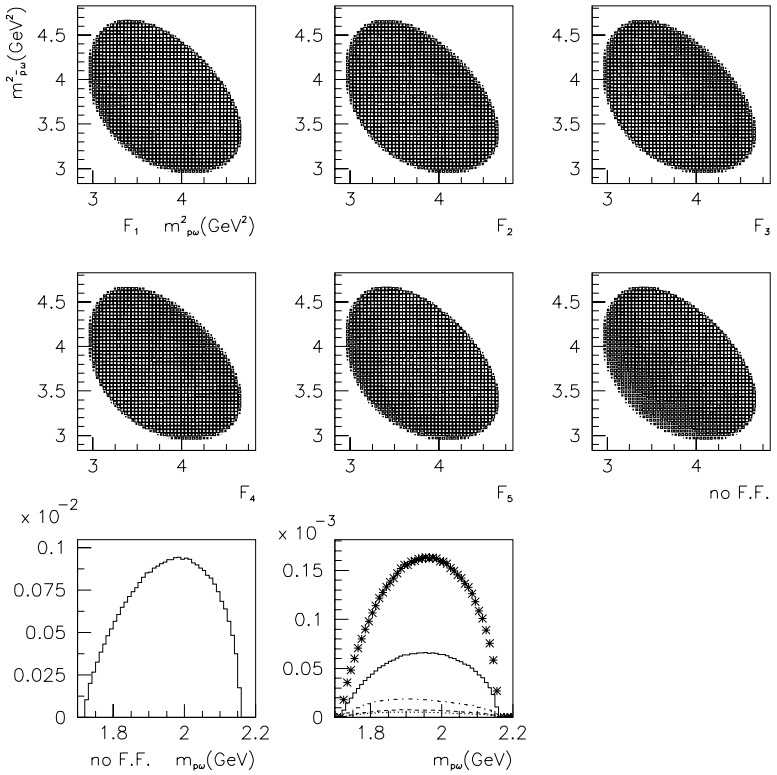

Fig. 12. The Dalitz plot and the $p\omega$ invariant-mass distribution in $J/\psi \to p\bar{p}\omega$ decay ($\Lambda = 1.5\,\mathrm{GeV}$). The solid, dashed, dotted, dot-dashed and starred curves denote the cases with F_1, F_2, F_3, F_4 and F_5, respectively.

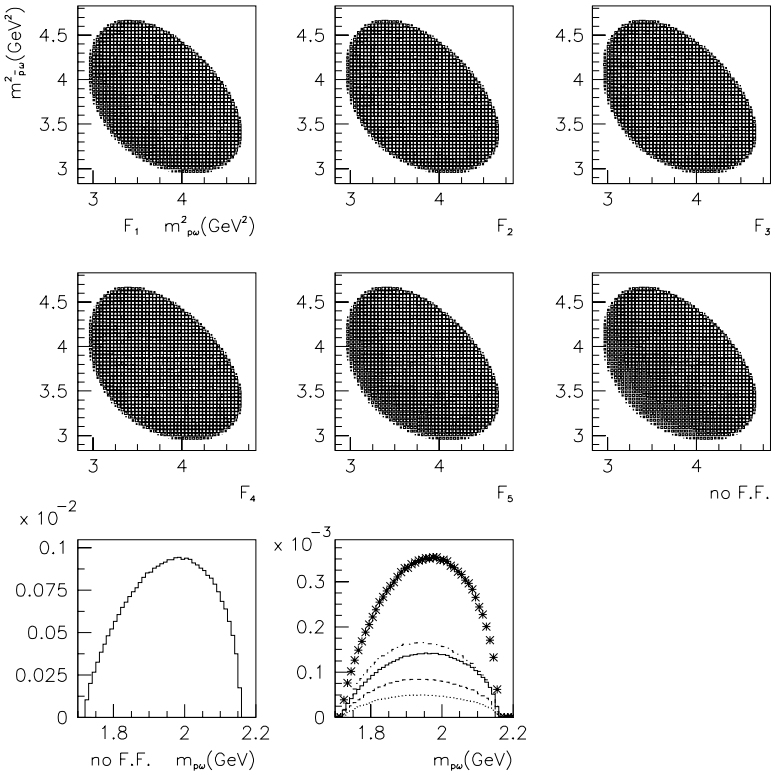

Fig. 13. The Dalitz plot and the $p\omega$ invariant-mass distribution in $J/\psi \to p\bar{p}\omega$ decay ($\Lambda = 2.0$ GeV). The solid, dashed, dotted, dot-dashed and starred curves denote the cases with F_1, F_2, F_3, F_4 and F_5, respectively.

The most Λ-sensitive form factor is F_3, with which the BR changes to almost 10^8 times as much when Λ increases from 0.65 GeV to 2.0 GeV. The most Λ-insensitive one is F_1, with which the BR only increases to 17 times as much. Moreover, when Λ is small, the BR is more sensitive to the form of the form factor. For instance, with $\Lambda = 0.65$ GeV, the resultant BRs from various form factors have almost a 10^9 times difference. But with $\Lambda = 2.0$ GeV, the difference is just about 3 times. The reason is the same as that in the $J/\psi \to p\bar{p}\pi^0$ case. We also provide the relevant Dalitz plot and the invariant-mass distribution of $p\omega$ in figs. 10-13. The Dalitz plot in these figures shows that the contributions of the proton-pole diagram in the high-momentum region are evidently suppressed. This agrees with our conjecture mentioned at the beginning of this section.

Furthermore, comparing with the data 0.61 ± 0.12 of PDG [9], we find that the resultant BRs are generally less by 10%. This indicates that in the $J/\psi \to p\bar{p}\omega$ decay, the proton-pole contribution is not so important. To explain the empirical data, there must be certain contributions from other diagrams such as the N^*-pole diagram.

4 Conclusion

$J/\psi \to N\bar{N}M$ decay is an ideal process to study the N^* spectrum. As intermediate states, nucleon and N^* can all contribute to the decay BR. In the $J/\psi \to N\bar{N}M$ decay data analysis, the nucleon-pole contribution would play an important role of background. Understanding this contribution would enable us to get a more accurate and more reliable information on N^*. In this paper, we study the nucleon-pole contribution by employing PS-PS and PS-PV $\pi N\bar{N}$ vertex couplings and various vertex form factors.

According to the equivalent theorem [24], the PS-PS and PS-PV couplings of the π-N interaction are equivalent, when the intermediate nucleon is on-shell. Namely, the decay amplitudes with the PS-PS and PS-PV coupling vertices are exactly the same. But, when the intermediate nucleon is off-shell, their decay amplitudes are different. The amplitude with the PS-PS coupling vertex keeps the same form as in the on-shell case, and the amplitude with the PS-PV coupling vertex has an additional term which describes a four-particle contact interaction. It seems that the PS-PV coupling contains the PS-PS coupling. In fact, many authors claimed that using the PS-PV coupling only is good enough in describing the π-N interaction and the meson photoproduction [13–15,25,26]. But some authors believed that a mixed coupling

$$g_{\pi NN}\tau_i \left[\lambda\gamma_5 - (1-\lambda)\frac{\not{p} - \not{p}'}{2m}\gamma_5\right], \qquad (51)$$

where λ is a mixing parameter, is more appropriate [11, 12,27]. The value of λ can be extracted by data fitting. For an example, Gross, Orden and Holinde [11] obtained $\lambda \cong 0.22$ by fitting the N-N data in a one-boson exchange (OBE) model, Goudsmit, Leisi and Mastinos found $\lambda \cong 0.24$ by analyzing the πN scattering data at the tree diagram level [27], Gross and Surya got $\lambda \cong 0.25$ by fitting the πN scattering data [12]. Anyway, the obtained λ value shows that in the mixed $NN\pi$ vetex, the PS-PS coupling only occupies a small portion.

Because the PS-PS and PS-PV couplings are not equivalent when the intermediate nucleon is off-shell, the resultant nucleon-pole contributions to $\Gamma(J/\psi \to p\bar{p}\pi^0)/\Gamma(J/\psi \to p\bar{p})$ in these cases are different. The smaller the $|F_0|/|F_M|$ ratio in the $J/\psi \to p\bar{p}$ decay is, the closer the BRs in the PS-PS and PS-PV cases are. For instance, when $|F_0|/|F_M| = 0.12$, the mentioned difference is quite small, and the ratio $\Gamma_{\rm PV}(J/\psi \to p\bar{p}\pi^0)/\Gamma_{\rm PS}(J/\psi \to p\bar{p}\pi^0)$ is about 0.94. The resultant BR is about 0.53. Comparing with the data value of 0.51, one can claim that the proton-pole diagram is the main contributor responsible for the BR of the $J/\psi \to p\bar{p}\pi^0$ decay.

On the other hand, the hadron has its own inner structure. To be realistic, one has to introduce vertex form factors. After considering the form factors, the mentioned BR difference is enlarged. The size of the change depends on the form of the form factor and its Λ value. In general, the smaller the Λ is, the large the difference will be. When Λ is small, say $\Lambda = 0.65$ GeV, the resultant BR of $J/\psi \to p\bar{p}\pi^0$ depends strongly on the form of the form factor. When the form factor takes an exponential form or a dipole form, it highly suppresses the contribution in the high-momentum part, and consequently, the resultant BR reduces to 0.08% or 0.4% of the value obtained without form factor. When Λ is large, say $\Lambda = 2.0$ GeV, all the form factors become very similar to each other, the form factor curves do not decrease too much, and then the resultant BRs are also very similar and are not small. They are about 20% to 30% of the value without form factor.

The Λ-sensitivity of the various form factors is also different. The exponential form factor is the most sensitive one. When the Λ value changes from 0.65 GeV to 2.0 GeV, the BR changes about 256 times as much. But for the most insensitive one (the monopole form factor), the change is only about 6 times as much.

Moreover, if one adopts a form factor that is frequently used in explaining the πN scattering and the pion photoproduction data, the proton-pole contribution is about 10–20% of the $J/\psi \to p\bar{p}\pi^0$ data. Thus, the proton-pole diagram must be considered.

The similar results for the $J/\psi \to p\bar{p}\eta$ and $p\bar{p}\eta'$ are studied in the same manner. Taking $|F_0|/|F_M| = 0.12$ and without considering the form factor, the resultant BRs from the proton-pole diagram are 5×10^{-4} and 2×10^{-4}, for the $J/\psi \to p\bar{p}\eta$ and $p\bar{p}\eta'$ decays, respectively. In comparison with the data values of 0.98 and 0.42, they are all less by 0.1%. Taking the form factor into account, the resultant BRs are further reduced. Therefore, in analyzing the $J/\psi \to p\bar{p}\eta$ and $p\bar{p}\eta'$ decay data, the contribution from the proton-pole diagram can safely be ignored.

The proton-pole diagram contribution to the $J/\psi \to p\bar{p}\omega$ decay is analyzed too. The difference between the resultant BRs by using vector coupling and mixed coupling is only about 3%. Comparing with the data value of 0.61, without considering the form factor and with

$|F_0|/|F_M| = 0.12$, the BR obtained from the proton-pole diagram is about 0.168, which is about 28% of the data value. When the form factor is considered, the largest obtained BR is less than 10% of the data value. This indicates that other diagrams such as the N^*-pole diagram may be mainly responsible for the $J/\psi \to p\bar{p}\omega$ decay.

Finally, it is worthy of note that through J/ψ decay data fitting, it is possible to select an appropriate form factor for the $J/\psi \to N\bar{N}M$ decay.

The authors would like to thank Professor Rahul Sinha for his fruitful discussion. We also thank Wei-Xing Ma for useful discussions. This work is partly supported by National Science Foundation of China under contracts Nos. 10075057, 90103020, 19991487, 10225525 and 10147202, the CAS Knowledge Innovation Key Project KJCX2-SW-N02, and the Deutsche Forschungsgemeinschaft.

Appendix A

In this appendix, we give the explicit expressions of $A_{\mathrm{PS},i}(i = 1, 2, 3)$ and $A_{\mathrm{PV},i}(i = 2, 3)$ appeared in eqs. (12) and (13),

$$\begin{aligned} A_{\mathrm{PS},1} = {} & \big(m^2 + p\cdot p'\big)\big[\big(a^2 - b^2\big)(\epsilon\cdot k)^2 + b^2\epsilon^2 k^2\big] \\ & - 2ab(\epsilon\cdot k)\big[(\epsilon\cdot p)\big(p'\cdot k\big) - \big(\epsilon\cdot p'\big)(p\cdot k)\big] \\ & - 2b^2\big[\epsilon^2(p\cdot k)\big(p'\cdot k\big) - (\epsilon\cdot k)\big(\epsilon\cdot p'\big)(p\cdot k) \\ & - (\epsilon\cdot k)(\epsilon\cdot p)\big(p'\cdot k\big) + k^2(\epsilon\cdot p)\big(\epsilon\cdot p'\big)\big], \end{aligned} \tag{52}$$

$$\begin{aligned} A_{\mathrm{PS},2} = {} & \frac{1}{m^2}\big[\big(m^2 - p\cdot p'\big)k^2 + 2(p\cdot k)\big(p'\cdot k\big)\big] \\ & \times\left[\frac{p'\cdot\epsilon}{2p\cdot k + k^2} - \frac{p\cdot\epsilon}{2p'\cdot k + k^2}\right]^2, \end{aligned} \tag{53}$$

$$A_{\mathrm{PS},3} = 4k^2\left[\frac{p'\cdot\epsilon}{2p\cdot k + k^2} - \frac{p\cdot\epsilon}{2p'\cdot k + k^2}\right]^2, \tag{54}$$

$$\begin{aligned} A_{\mathrm{PV},2} = {} & \frac{1}{m^2}\big(p\cdot\epsilon - p'\cdot\epsilon\big)\left(\frac{p'\cdot\epsilon}{2p\cdot k + k^2} - \frac{p\cdot\epsilon}{2p'\cdot k + k^2}\right) \\ & \times\big(p\cdot k + p'\cdot k\big) + \frac{1}{4m^4}\big(m^2 + p\cdot p'\big)\big(p\cdot\epsilon - p'\cdot\epsilon\big)^2, \end{aligned} \tag{55}$$

$$\begin{aligned} A_{\mathrm{PV},3} = {} & \frac{1}{m^2}\big(p\cdot\epsilon - p'\cdot\epsilon\big)\big\{a\,\big(m^2 + p\cdot p'\big)(k\cdot\epsilon) \\ & + b\,\big[\big(p'\cdot\epsilon\big)(p\cdot k) - (p\cdot\epsilon)\big(p'\cdot k\big)\big]\big\}, \end{aligned} \tag{56}$$

where we have set for simplicity

$$a = \frac{1}{2p\cdot k + k^2} - \frac{1}{2p'\cdot k + k^2}, \tag{57}$$

$$b = \frac{1}{2p\cdot k + k^2} + \frac{1}{2p'\cdot k + k^2}. \tag{58}$$

References

1. V.D. Burkert, Nucl. Phys. A **623**, 59c (1997); Prog. Part. Nucl. Phys. **44**, 273 (2000).
2. N. Isgur, G. Karl, Phys. Lett. B **72**, 109 (1977); Phys. Rev. D **23**, 817 (1981).
3. D. Faiman, W. Hendry, Phys. Rev. **173**, 1720 (1968); **180**, 1609 (1969).
4. S. Capstick, P.R. Page, Phys. Rev. D **60**, 111501 (1999); nucl-th/0008028.
5. B.S. Zou, Nucl. Phys. A **675**, 167 (2000); **684**, 330 (2001).
6. B.S. Zou, H.B. Li, BES Collaboration, in *Excited Nucleons and Hadronic Structure, Proceedings of NSTAR2000 Conference at Jefferson Lab*, edited by V. Burkert *et al.* (World Scientific, 2001) p. 155, hep-ph/0004220; H.B. Li *et al.*, Nucl. Phys. A **675**, 189 (2000).
7. R. Sinha, Susumu Okubo, Phys. Rev. D **30**, 2333 (1984).
8. DM2 Collaboration, Nucl. Phys. B **292**, 653 (1997).
9. Particle Data Group, Euro. Phys. J. C **15**, 1 (2000).
10. R. Machleidt, K. Holinde, Ch. Elster, Phys. Rep. **149**, 1 (1987); R. Machleidt, Adv. Nucl. Phys. **19**, 189 (1989); G. Holzwarth, R. Machleidt, Phys. Rev. C **55**, 1088 (1997).
11. F. Gross, J.W. Van Orden, K. Holinde, Phys. Rev. C **45**, 2094 (1992); **41**, R1909 (1990).
12. F. Gross, Y. Surya, Phys. Rev. C **47**, 703 (1993).
13. B.C. Pearce, B.K. Jennings, Nucl. Phys. A **528**, 655 (1991).
14. C. Schütz, J.W. Durso, K. Holinde, J. Speth, Phys. Rev. C **49**, 2671 (1994).
15. T. Sato, T.-S.H. Lee, Phys. Rev. C **54**, 2660 (1996).
16. Q. Zhao, Z. Li, C. Bennhold, Phys. Rev. C **58**, 2393 (1998); Q. Zhao, J.-P. Didelez, M. Guidal, B. Saghai, Nucl. Phys. A **660**, 323 (1999); Q. Zhao, B. Saghai, J.S. Al-Khalili, Phys. Lett. B **509**, 231 (2001).
17. Q. Haider, L.C. Liu, J. Phys. G **22**, 1187 (1996); L.C. Liu, W.X. Ma, J. Phys. G **26**, L59 (2000).
18. L.L. Frankfurt, M. Strikman, Z. Phys. A **334**, 343 (1989).
19. V.G.J. Stoks, R.A.M. Klomp, C.P.F. Terheggen, J.J. de Swart, Phys. Rev. C **49**, 2950 (1994).
20. H. Haberzettl, C. Bennhold, T. Mart, T. Feuster, Phys. Rev. C **58**, R40 (1998).
21. Y. Oh, A. Titov, T.-S.H. Lee, Phys. Rev. C **63**, 25201 (2001).
22. T. Yoshimoto, T. Sato, M. Arima, T.-S.H. Lee, Phys. Rev. C **61**, 65203 (2000).
23. Y. Oh, A.I. Titov, T.-S.H. Lee, presented at the *NSTAR 2001 Workshop on the Physics of Excited Nucleons, Mainz, Germany, 7-10 March 2001*, nucl-th/0104046.
24. G.F. Chew, Phys. Rev. **95**, 1669 (1954).
25. R.D. Peccei, Phys. Rev. **176**, 1812 (1968).
26. C. Lee, S.N. Yang, T.-S.H. Lee, J. Phys. G **17**, L131 (1991).
27. P.F.A. Goudsmit, H.J. Leisi, E. Mastinos, Phys. Lett. B **299**, 6 (1993); Report No. ETHZ-IMP PR/91-6, 1991.